Cell

Rapid Telomere Movement in Meiotic Prophase Is Promoted By *NDJ1*, *MPS3*, and *CSM4* and Is Modulated by Recombination

Michael N. Conrad,[1,5] Chih-Ying Lee,[1,2,5] Gene Chao,[1] M. Shinohara,[3] H. Kosaka,[3] A. Shinohara,[3] J.-A. Conchello,[1,4] and Michael E. Dresser[1,2,*]

[1]Program in Molecular, Cell and Developmental Biology, Oklahoma Medical Research Foundation, Oklahoma City, OK 73104, USA
[2]Department of Cell Biology, Oklahoma University Health Sciences Center, Oklahoma City, OK 73104, USA
[3]Division of Integrated Protein Functions, Institute for Protein Research, Osaka University, Osaka, Japan 4
[4]Department of Electrical Engineering, Oklahoma University, Norman, Oklahoma 73019, USA
[5]These authors contributed equally to this work
*Correspondence: dresserm@omrf.ouhsc.edu
DOI 10.1016/j.cell.2008.04.047

SUMMARY

Haploidization of the genome in meiosis requires that chromosomes be sorted exclusively into pairs stabilized by synaptonemal complexes (SCs) and crossovers. This sorting and pairing is accompanied by active chromosome positioning in meiotic prophase in which telomeres cluster near the spindle pole to form the bouquet before dispersing around the nuclear envelope. We now describe telomere-led rapid prophase movements (RPMs) that frequently exceed 1 μm/s and persist throughout meiotic prophase. Bouquet formation and RPMs depend on *NDJ1*, *MPS3*, and a new member of this pathway, *CSM4*, which encodes a meiosis-specific nuclear envelope protein required specifically for telomere mobility. RPMs initiate independently of recombination but differ quantitatively in mutants that fail to complete recombination, suggesting that RPMs respond to recombination status. Together with recombination defects described for *ndj1*, our observations suggest that RPMs and SCs balance the disruption and stabilization of recombinational interactions, respectively, to regulate crossing over.

INTRODUCTION

Faithful haploidization of the genome during gamete formation requires that homologous chromosomes (homologs) join in pairs in meiotic prophase, undergo allelic recombination, and then disjoin from one another in the first meiotic division. A central question of meiosis is how DNA transactions are coordinated with chromosome mechanics to generate and regulate crossing over (see Kleckner et al., 2004; Bishop and Zickler, 2004). Roughly coincident with the onset of pairing and synapsis, telomeres congregate at a small region of the nuclear envelope (NE) adjacent to the spindle pole to form the chromosome bouquet. Bouquet formation is conserved evolutionarily and may promote pairing by bringing chromosomes close together and in register (Zickler, 2006). Chromosome movements thought to be related to bouquet formation occur in diverse species—rat, cricket, *S. pombe* (reviewed in Zickler and Kleckner, 1998), and *S. cerevisiae* (Trelles-Sticken et al., 2005). Telomere movements in *S. cerevisiae* depend in part on Ndj1p (Scherthan et al., 2007), which functions with SUN domain protein Mps3p to form the bouquet (Conrad et al., 2007). SUN domain proteins also are required for or have been implicated in normal meiotic telomere behavior in *S. pombe* (Miki et al., 2004; Shimanuki et al., 1997; Chikashige et al., 2006), mouse (Ding et al., 2007; Schmitt et al., 2007), and *C. elegans* (Penkner et al., 2007). SUN domain proteins are widely implicated in bridging the NE to link nucleus with cytoskeleton and may serve to link meiotic chromosomes to motive forces generated by association with microtubules (Chikashige et al., 2007) or actin filaments (Trelles-Sticken et al., 2005; Koszul et al., 2008).

We have found that rapid telomere-led movements initiate early in meiotic prophase and continue until just prior to first meiotic metaphase. Using new methods to analyze these "rapid prophase movements" (RPMs), we find that they can exceed speeds of 1 μm/s, are dependent on *NDJ1* (Conrad et al., 1997; Chua and Roeder, 1997), *MPS3* (Conrad et al., 2007), and a new member of the bouquet pathway, *CSM4*, and are modulated by but not dependent on meiotic recombination.

RESULTS

Rapid Meiotic Prophase Movements of Chromosomes Are Heterogeneous

We examined the movements of entire chromosomes by using Rec8-GFP, a meiosis-specific cohesin, to label chromosome axes during meiotic prophase (Klein et al., 1999). Visualized using a spinning disk confocal microscope, chromosomes appear to move independently, with some chromosomes moving while others remain relatively stationary (Figure 1A, Movie S1 available online). To visualize chromosome ends specifically, we fused GFP to Mps3p, which localizes to telomeres during meiotic

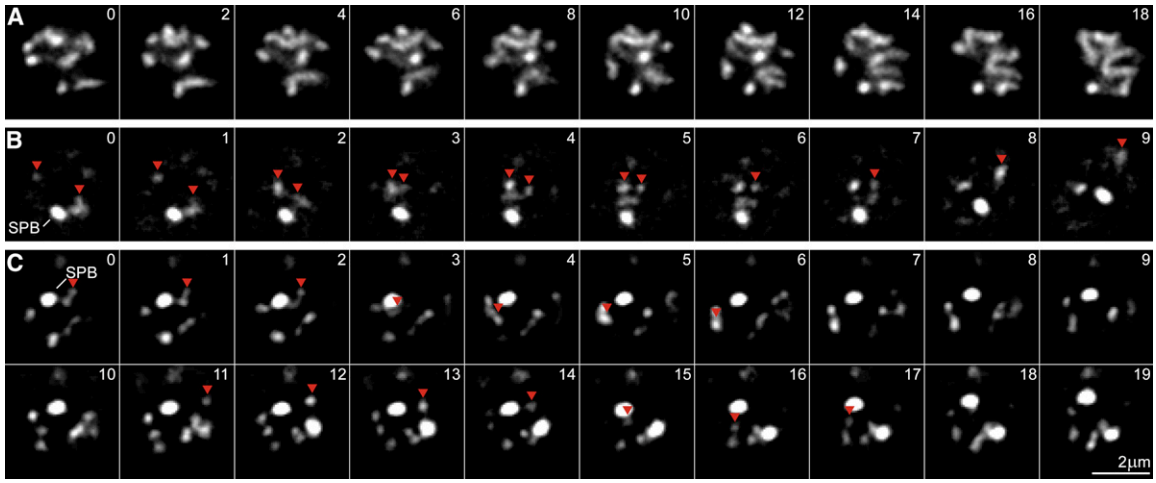

Figure 1. Chromosome Movements in Meiotic Prophase Are Independent, Rapid, and Heterogeneous

Confocal timelapse images of individual nuclei where chromosome axes are labeled with Rec8-GFP (A, equatorial plane) or the spindle pole body (SPB) and telomeres are labeled with Mps3-GFP (B and C, tangential planes). Numbers at the upper right of each panel represent seconds. Red arrowheads mark rapidly moving Mps3 spots.

(A) Most chromosomes move in and out of the plane of focus, but some appear relatively stable (e.g., the spot at bottom, center, shows no lateral movement).

(B) Two spots, likely representing telomere clusters, collide and then one moves to upper right, accompanied at a distance by the SPB, while the other remains stationary.

(C) Two spots, at different times (1–6 s and 11–16 s), move along a similar path by the SPB.

prophase (as well as to the spindle pole body [SPB]) (Conrad et al., 2007). Telomeres (or clusters of telomeres) generally move relatively slowly, 0.3 μm/s or less, but occasionally move in excess of 1 μm/s (Figures 1B and 1C, Movie S1). The most rapid movements frequently appear to end with elastic recoil and to disrupt telomere clusters. Independent movements along a similar path (Figure 1C) suggest tracks for the movements, although simultaneous movements in nearly opposite directions and successive orthogonal movements indicate an underlying complexity (Figure 5B).

Quantification of RPMs using Thru-Focus Imaging

To evaluate RPMs quantitatively, we imaged the movements of individual parts of chromosomes tagged with GFP spots. Conventional imaging approaches are limited in tracking GFP spots that quickly are lost from view in single focal plane timelapse acquisitions (Movie S2, "single plane") and move across focal planes during the acquisition of image stacks. We developed a new imaging approach to minimize these problems (Conchello and Dresser, 2007). In this method, a single exposure is made while moving focus through the specimen. Deconvolution removes blur in the 2D "projection" image (Movie S2, "thru-focus"). The ability to image large numbers of cells compensates for the loss of information about localization along the Z axis. All timelapse acquisitions for visualization of GFP spots were acquired at 1 frame per second with exposures of 250 ms per frame, for 60 frames (see Experimental Procedures and Movie S3).

We constructed isogenic diploid strains with concatemers of *lacI-GFP* binding sites at (1) the right telomere of chromosome *IV* (*IVR* TEL), (2) the left telomere of chromosome *VII* (*VIIL* TEL), (3) the left telomere of chromosome *III* (*IIIL* TEL), (4) the centromere of chromosome *VII* (*VII* CEN), or (5) the middle of the left arm of chromosome *VII* (*VIIL* MID). Tubulin-GFP marked the SPB, which appears as a larger, less discrete spot. Both homologs were tagged to evaluate whether the sites were paired (single, fused GFP spot) or unpaired (two spots). In vegetative and premeiotic cells, some pairing likely represents chance overlap of the signals, or inclusion of the two telomeres in a cluster at the NE (Klein et al., 1992). At later time points in wild-type (WT) cells, the majority of paired spots likely result from homologous synapsis.

In meiotic cells the RPMs of individual loci are obviously more extensive than movements in vegetative or premeiotic cells (compare movements at 1 to 5 hr in sporulation medium, Movie S4). To quantify movements, the location of each spot was determined in each frame for ~100 cells sampled at each hour (examples in Figures 2A–2C). The velocities and extents of travel are represented by five parameters calculated for each spot on the projected 2D image: (1) the average speed, in microns per second, (2) the maximum speed out of 59 measures, in microns per second, (3) the standard deviation of the 59 speeds measured for each spot, (4) the directional bias, calculated as the average of the cosines of the angles made by the pairs of vectors representing successive movements (bias is ~0 for random movement, <0 for tendency to remain in place and >0 for tendency to move away from the starting position), and (5) the area of the bounding box required to enclose all positions of the spot. "Bias" is adapted from measures of bacterial motility (see Berg, 1993). In simple terms, the first two parameters describe how fast the spots move and the last two parameters describe how far the spots move (examples in Figure 2C).

Nuclei are approximately spherical in cross-section even though the RPMs clearly cause some deformations (Hayashi et al., 1998); see WT in Movie S6). To provide context for

interpreting the experimental results, Monte Carlo simulations were generated by moving spots along spherical surfaces and projecting the spot positions onto a 2D plane representing the camera pixels. These synthetic data generally fit well with experimental data (see the Supplemental Experimental Procedures).

RPMs Coincide with Meiotic Prophase I

The largest increases in telomere movements were seen in cells with paired telomeres at 4 and 5 hr after the shift into sporulation medium, coincident with meiotic prophase (Figures 2D–2G and Table S1). The movements return almost to 0 hr levels at 5 hr in nuclei that have entered first meiotic metaphase, as marked by the presence of a spindle (the "MI" data points in Figures 2D–2G). Movements of the SPB during meiotic prophase in *S. cerevisiae* are limited and, although the movements are more directed in meiotic prophase as measured by the bias (Figure 2G), we do not observe a stage resembling the *S. pombe* "horsetail" in which the whole nucleus is pulled back and forth in the cell continually (Chikashige et al., 1994; Miki et al., 2002). Closer examination of the bias distributions reveals that the increase for the paired telomeres is relatively large and discrete (Figure 2H) and a smaller increase is seen for the SPB (Figure 2I). Thus, the gradually increasing averages depicted in Figures 2D–2G presumably result from increasing fractions of cells in meiotic prophase. These results show that the RPMs are unique to meiotic prophase and are independent of SPB or of whole nuclear movements.

Unpaired and Paired Telomeres Exhibit RPMs

Chromosomes generally are unpaired in premeiotic cells, so that measurements of unpaired spots are disproportionately affected by asynchrony and nonsporulating cells (~10%) in the cultures. Because SPB bias increases during meiotic prophase, we compared the paired telomere values to unpaired telomere values from only those cells with SPB bias at or above −0.2, thus enriching for cells that have entered prophase (Figure 2I). Unpaired and paired telomeres in meiotic prophase move at similar average speeds (Figure 3A) even though some unpaired telomeres show a lower bias to their movements than do the paired telomeres (Figure 3B). The maximum speed distribution for paired telomeres shows peaks representing speeds of 0.45–0.6 and 0.75–0.9 microns per second (Figure 3C, "1" and "2"; smaller peaks are occasionally seen at higher values) while the unpaired telomeres show only the first peak. These peaks do not coincide with spacing of the camera pixels and are unlikely to result from artifacts in the imaging or analytical methods. These fast movements are intermittent, consistent with what is observed subjectively, but occur in a large fraction of cells over the course of only one minute.

RPMs Largely Are Independent of Locus or Chromosome Size

To determine whether RPM characteristics are general or locus dependent, perhaps influenced by chromosome size, we compared movements of telomeres *IIIL*, *IVR*, and *VIIL*. The patterns and absolute values of the RPMs for telomeres *IIIL*, *IVR*, and *VIIL* are similar (Figures 3D–3F), except that *IIIL* exhibits a 0.3 μm/s peak ("v," for values 0.15–0.3 μm/s). This peak coincides with the single peak seen for paired telomeres in non-prophase cells (data not shown) and presumably represents Brownian motion. Delayed onset of chromosome *III* RPMs may account for this observation.

RPMs Are Led by the Telomeres

We compared the movements of interstitial sites on chromosome *VII* with telomere *VIIL* movements. The centromere and the middle of the left arm of chromosome *VII* (Conrad et al., 2007) (1) show RPMs in meiotic prophase (Table S1), (2) move considerably slower than the *VIIL* telomere even when paired and presumably synapsed (Figures 3G and 3H), and (3) move similarly, suggesting that the centromere does not actively contribute to the RPMs. Also, the relatively high biases for the interstitial loci (Figure 3I) are consistent with whole chromosomes tending to move away from their starting positions (see Movie S1).

The Fastest RPMs Occur in Early Prophase

The 0.9 μm/s maximum speed is prevalent at 4 but not at 5 hr, suggesting that it specifically occurs early in prophase. As a test, we measured telomere movements at a relatively late time point in *ndt80Δ* mutants that fail to exit prophase. Surprisingly, the 0.9 μm/s peak persists in *ndt80Δ* at 7 hr (Figure 3J). In *ndt80Δ*, cells block in pachytene with complete SCs (Xu et al., 1995) and, although reciprocal recombination proceeds through formation of double Holliday junctions, double-strand breaks (DSBs) are continually made and turned over (Allers and Lichten, 2001). In WT cells, recombination intermediates upstream of double Holliday joins disappear as chromosomes synapse. To examine cells that are likely to have these intermediates in the WT dataset, we selected cells with telomeres that are "nearly paired," i.e., are unpaired but in close proximity in most frames of the timelapse acquisition. We analyzed separately those nuclei where over one minute the mean distance between homologous telomeres *IVR* was <0.4 μm versus ≥0.4 μm (Figure 3K). The curves for these "nearly paired" and paired telomeres at 4 hr are almost identical, consistent with the possibility that a recombination intermediate triggers 0.9 μm/s bursts and ruling out the possibility that the 0.9 μm/s peak requires stably synapsed telomeres.

Meiotic Recombination Is Not Required for RPMs

We began testing the role of recombination in the RPMs by examining *spo11Δ*. Spo11p forms the DNA DSBs that initiate recombination (Keeney et al., 1997). In *spo11Δ*, the frequency of paired telomeres *IVR* remains low in meiotic prophase, as expected (Table S1). Unpaired telomere RPMs in *spo11Δ* (and in the nuclease-deficient $spo11^{Y135F}$, data not shown) are similar to the RPMs in WT (Figure 4A; Table S1). Because the movements in *spo11Δ* appeared slightly less robust than in WT, and the kinetics of meiosis are altered in *spo11Δ* (Cha et al., 2000), we tested whether duration in meiotic prophase might alter the movements. We found that at 7 hr, unpaired telomeres in the *ndt80Δ spo11Δ* double mutant move considerably faster than unpaired telomeres in *spo11Δ* or WT at 4 hr (Figure 4A), reaching levels that resemble paired WT telomeres (Table S1) but without a peak at 0.9 μm/s (Figure 4B). These observations are consistent with a role for recombination intermediates in modulating

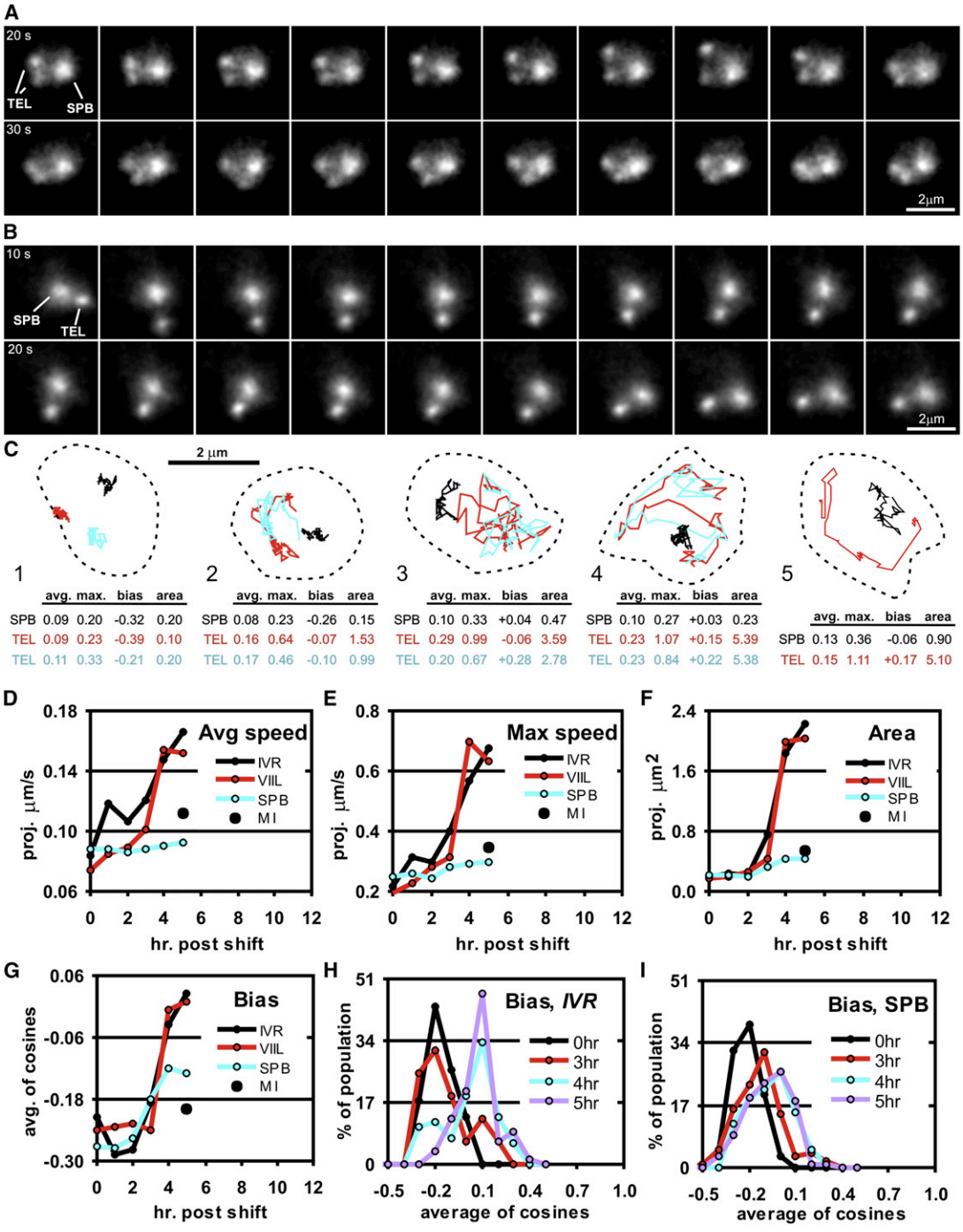

Figure 2. Telomeres Move Rapidly throughout Meiotic Prophase I

Thru-focus images of single cells, cropped from a timelapse series that captured data at 1 frame/s for ~200 WT cells at once (A and B), traces for spot movements in individual cells (C), and measurements of movement characteristics for ~100 cells per time point for each spot/site, where each cell is imaged for 1 min at 1 frame/s (D–I). Each data point in (D)–(G) represents 960 to10,080 measurements. Chromosome movements that occurred when the SPB moved >0.2 μm in 1 s were omitted to reduce the impact of whole-nucleus movements.

(A) Chromosome *IVR* telomeres ("TEL") are marked by relatively small, discrete *lacO*$_{256}$/*lacI-GFP* spots and are unpaired so that two spots are evident (at the left in each frame) until they overlap at t = 44 s. The spindle pole body ("SPB") is marked by Tub1-GFP, providing a spot that appears larger and fuzzier (to the right of the telomere spots in each frame).

(B) From the same dataset as in (A), images of a different cell where the telomeres are paired, giving rise to a single spot that moves clockwise around the relatively stationary SPB.

RPMs, although clearly the RPMs in general are independent of the initiation of recombination.

Defects in Recombination Alter RPMs

We next examined RPMs in *rec8Δ*, *dmc1Δ*, and *zip1Δ*, each of which blocks in meiotic prophase in our strain background. Rec8p is a meiosis-specific cohesin required for axial element formation and synapsis. In *rec8Δ*, DSBs generally fail to turn over and crossovers form at very low levels (Klein et al., 1999). Dmc1p is a recA-like recombinase required to generate stable strand invasion intermediates (Bishop et al., 1992). In *dmc1Δ*, DSBs fail to turn over but axial elements form (Bishop et al., 1992; Dresser et al., 1997) and, after some delay, chromosomes synapse (Rockmill et al., 1995). Zip1p forms the central region of the SC and is required for synapsis but not for axial element formation (Sym et al., 1993). In *zip1Δ*, DSBs turn over, single-end invasion intermediates (SEIs) accumulate slowly but to relatively high levels, and crossovers form at very low levels (Borner et al., 2004).

At 7 hr, unpaired *IVR* telomeres in *rec8Δ*, *dmc1Δ*, and *ndt80Δ spo11Δ* all show similar distributions in the maximum speed histograms, and ~30% of the values for each are higher than seen in *ndt80Δ* (Figure 4B). Maximum speed values for paired telomeres in *rec8Δ* and *dmc1Δ* show peaks at ~peak 1 (Figure 4C), similar to their unpaired telomere values. These similarities in *rec8Δ* and *dmc1Δ* extend to other measures as well (Table S1). Maximum speeds for unpaired and paired telomeres in *zip1Δ* and for paired telomeres in *ndt80Δ* all show peaks at ~peak 2 (Figure 4D) even though the area, average speed, and bias values are all higher for *zip1Δ* than for *ndt80Δ* (Table S1). Synapsis is absent even for the paired telomeres in *zip1Δ* and thus is not required for peak 2, consistent with the results from WT cells (Figure 3). These results suggest that a recombination intermediate that follows DSB turnover, or perhaps axial associations per se (Rockmill et al., 1995; Fung et al., 2004), induce more robust RPMs and that the robust RPMs continue until the intermediate is turned over or until a later event halts them. Unpaired telomere movements at 0.9 μm/s and above are infrequent in *ndt80Δ* at 7 hr (Figure 4B and data not shown), suggesting that the more robust RPMs either were never initiated or were turned off for these telomeres or nuclei.

Bouquet Genes Are Required for Normal RPMs and Chromosome Distribution

CSM4 Is a New Bouquet Gene

NDJ1 (Trelles-Sticken et al., 2000) and *MPS3* (Conrad et al., 2007) each are required for bouquet formation and additional meiotic events, and *NDJ1* is required for normal meiotic chromosome movements (Scherthan et al., 2007). Csm4p is a meiosis-specific, tail-anchored membrane protein (Beilharz et al., 2003). Absence of Csm4p causes defects in meiotic chromosome segregation (Rabitsch et al., 2001) similar to those seen in the absence of Ndj1p or of an N-terminal domain of Mps3p that interacts with Ndj1p (*mps3*$^{\Delta 2\text{-}64}$; Conrad et al., 2007). In *csm4Δ*, bouquet formation is defective, pairing is delayed, and chromosome missegregation is elevated, each at levels similar to those in *ndj1Δ* (Figure S1). In *rec8Δ*, cells arrest in meiotic prophase with a single large telomere cluster (Trelles-Sticken et al., 2005), but *rec8Δ ndj1Δ* cells lack the telomere cluster at the arrest (Conrad et al., 2007). Telomeres similarly fail to cluster in *rec8Δ csm4Δ* (data not shown). These observations establish *CSM4* as a bouquet gene with functions similar to those of Ndj1p and Mps3p. However, there are differences in the requirements for Ndj1p and Csm4p. With respect to *ndj1Δ*, onset of anaphase I in *csm4Δ* is delayed an additional 2 hr and spore formation and viability (in 4-spored asci) is more defective (Figure S1). Interestingly, *ndj1Δ* fails to suppress the anaphase I onset delay but partially suppresses both spore formation and viability in *csm4Δ* (Figure S1; spore viability is 92% in WT, 62% in *ndj1Δ*, 43% in *csm4Δ*, and 56% in *ndj1Δ csm4Δ*).

Bouquet Genes Promote RPMs

We visualized chromosome movements in *ndj1Δ*, *mps3*$^{\Delta 2\text{-}64}$ and *csm4Δ* cells in meiotic prophase using a spinning disk confocal microscope. Telomere movements are reduced in each of these mutants (Movie S5). In WT, the chromosomes frequently are peripheral in the nucleus (White et al., 2004), while in *ndj1Δ* and *mps3*$^{\Delta 2\text{-}64}$ the chromosomes generally are more evenly distributed throughout the nucleus (Figures 5A–5C), consistent with a defect in telomere attachment to the NE (Trelles-Sticken et al., 2000; Conrad et al., 2007). In *csm4Δ* (Figure 5D), nuclei with peripheralized chromosomes accumulate during the long delay in meiotic prophase, while in *ndj1Δ csm4Δ* (Figure 5E) chromosomes appear distributed as in *ndj1Δ*. Single, equatorial plane movies of Mps3-GFP non-SPB spots show the expected movements in WT cells and relative immobility in *csm4Δ* (Movie S6). In *ndj1Δ* and *ndj1Δ csm4Δ*, Mps3-GFP signal remains in the nuclear envelope, but spots are less apparent and motion is difficult to assess; nuclei are particularly round in cross-section and unperturbed by movements in *csm4Δ* and *ndj1Δ csm4Δ* (Movie S6). Therefore, unlike Ndj1p and Mps3p, Csm4p appears not to be required to anchor telomeres to the NE. The absence of RPMs in *ndj1Δ* and *mps3*$^{\Delta 2\text{-}64}$ may result from failure of the telomeres to form a stable association with the NE, while *csm4Δ* may prevent telomere association with the machinery that provides force for the movements. *Ndj1Δ* may partially suppress *csm4Δ* by

(C) Traces of the movements of SPB (black) and TEL (red and blue) spots in 60-frame timelapse series from five cells. The traces in 2 and 5 are of the cells depicted in (A) and (B), respectively. Relatively faint background fluorescence, presumably from unbound GFP-tagged proteins, marks the extent of each nucleus (too faint to be visible in A and B). The dashed lines enclose the projection image of this fluorescence for all 60 frames. These boundaries estimate the limits of the nuclear periphery, which undergoes some deformations, presumably related to the movements, during acquisition of the series. Measures tabulated for each spot, in each nucleus, are the speed average, speed maximum, directional bias, and area covered.

(D–G) Average values for ~100 cells taken each hour from 0 to 5 hr after inducing meiosis and sporulation. Plotted are the average speed, maximum speed, area, and bias measures for paired telomeres at chromosomes *IVR* and *VIIL* and for the SPB from the *IVR* dataset. The *IVR** data point is for nuclei at 5 hr that contain a metaphase I spindle.

(H) Histogram of bias values for paired (single spot) telomeres *IVR* at 0, 3, 4, and 5 hr, showing a discrete increase in the bias and increasing fractions of cells in meiotic prophase from 3 to 5 hr.

(I) Histogram of bias values for the SPB at 0, 3, 4, and 5 hr, showing a clear but less apparently discrete increase than seen for the telomeres in (H).

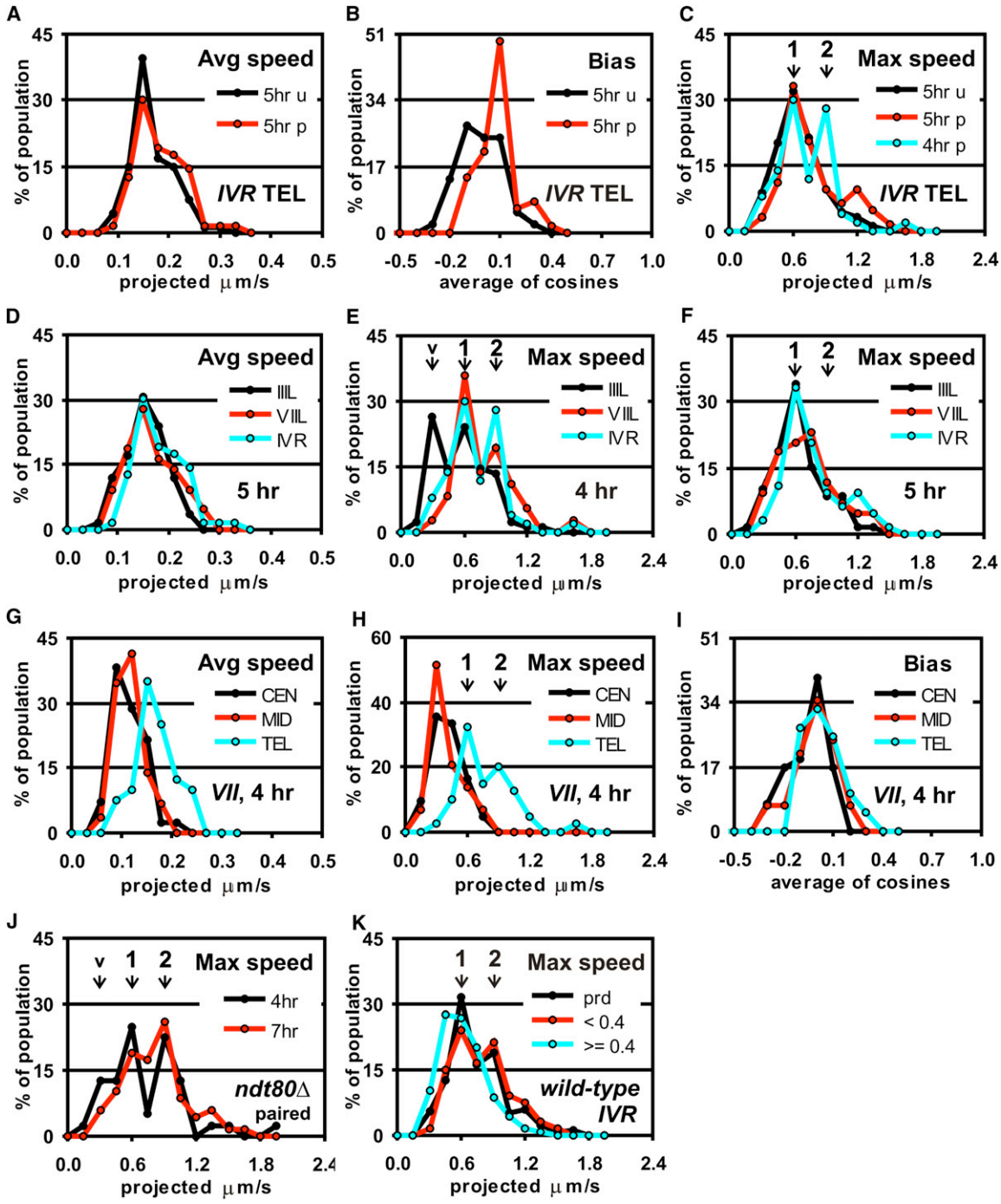

Figure 3. Movements of Unpaired and Paired Telomeres and Interstitial Chromosome Sites Differ in Detail

Histograms of values from cells that had SPB bias measures in excess of −0.2, to reduce contributions from nonprophase cells (numbers of measurements in Table S1).

(A–C) Histograms of values for unpaired ("u") and paired ("p") telomeres *IVR* in WT cells taken at 4 and 5 hr in sporulation. In meiotic prophase, unpaired telomeres move with the same average speed as paired telomeres and show the same maximum speed peak at 0.6 μm/s ("1") but can have a lower bias and do not show the maximum speed peaks at 0.9 and 1.2 μm/s ("2" and "3") seen for the paired telomeres.

(D–F) Histograms for paired telomeres at *IIIL*, *IVR*, and *VIIL* at 4 and 5 hr in sporulation. The peak in the maximum speed graph at 0.3 μm/s for *IIIL* ("v") also is characteristic of all paired telomeres in nonmeiotic prophase cells. Different telomeres move with similar average speeds, develop maximum speed peaks 1 and 2 at 4 hr, and lose peak 2 but develop faster speeds at 5 hr. Peak 3 may not develop for telomeres *IIIL*, which appear to lag in beginning the prophase movements.

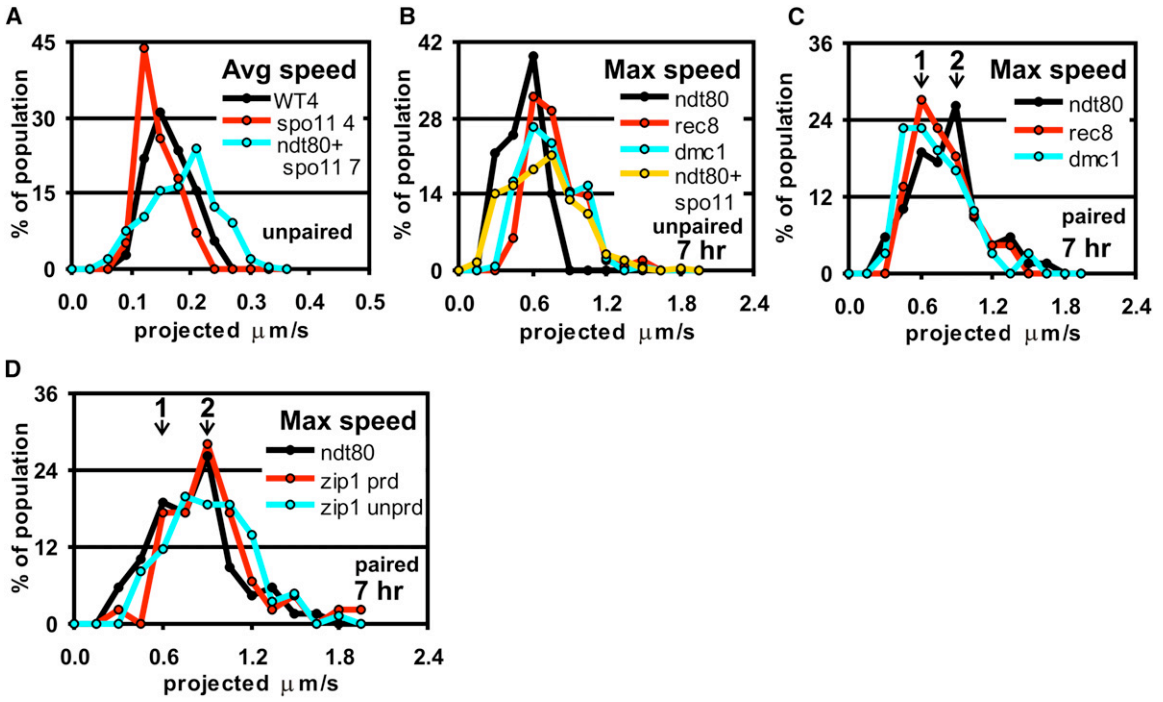

Figure 4. Rapid Telomere Movements Are Influenced by Meiotic Recombination

Histograms of telomere *IVR* movements for cells in meiotic prophase (SPB bias > −0.2; numbers of measurements in Table S1).

(A) Telomere movements in *spo11Δ* at 4 hr (spo11 4) are slower on average than in wild-type (WT 4) but become relatively rapid in *spo11Δ* when held in prophase by *ndt80Δ* (ndt80+spo11 7).

(B) Maximum speed values for unpaired telomeres at 7 hr in *ndt80Δ* show a strong peak at 0.6 μm/s (peak 1 in Figure 3) while increased numbers of cells with higher values are seen in *rec8Δ*, *dmc1Δ*, and *ndt80Δ spo11Δ*.

(C) Maximum speed values for *rec8Δ* and *dmc1Δ* show peak 1 but not peak 2 (*ndt80Δ* values as shown in Figure 3J).

(D) Maximum speed values for paired telomeres at 7 hr in *zip1Δ* are nearly identical to those of *ndt80Δ*, and the unpaired telomeres in *zipΔ* show a broad peak that also is centered at 0.9 μm/s.

weakening telomere association with an immobile NE attachment (see Figure S1).

Telomere *IVR* movements were assessed in *ndj1Δ*, *mps3*$^{\Delta 2\text{-}64}$, *csm4Δ*, and *ndj1Δ csm4Δ* at 4 hr for early meiotic prophase and at 7–8.5 hr to allow SCs to form. At 8.5 hr, paired telomere movements in *csm4Δ* (Figures 5F–5H) resemble WT at 0 hr (Table S1) with bias levels below even the SPB (Table S1). In these assays, *mps3*$^{\Delta 2\text{-}64}$ is virtually identical to *csm4* (Table S1, data not shown). Telomere movements in *ndj1Δ* are significantly lower than WT levels in average speed, bias, and maximum speed (Figures 5F–5H, Table S1) but do show a mild increase at 7 hr (Table S1). Telomere movements in *ndj1Δ csm4Δ* are at near *csm4Δ* levels, suggesting that *CSM4* is epistatic to *NDJ1* in this regard (although *ndj1Δ* appears to slightly suppress *csm4Δ*; Table S1). In all the mutants, paired telomeres move slower than unpaired telomeres, the reverse of what is seen in meiotic prophase WT cells (Table S1). Presumably, in the absence of the RPMs, being synapsed or clustered restrains telomere mobility, perhaps because the combined mass reduces Brownian motion-type movements. These observations suggest a model where Ndj1p promotes telomere association with Mps3p, which anchors telomeres to the NE, and Csm4p promotes connection to forces that generate RPMs.

Chromosome Distribution Is Altered in Bouquet Gene Mutants

We assayed the effects of movement defects on the position of individual telomeres relative to the SPB in each frame of the time-lapse datasets. The results were compared to synthetic data where telomeres could be restricted to areas defined with respect to the SPB (to model the effect of the Rabl orientation (Bystricky et al., 2005) in spheres of different diameters (to model the effects of changing nuclear size during meiotic prophase).

We found a shift from a mitotic (Figure 5I) to a meiotic (Figure 5J) distribution as cells proceed through meiotic prophase in WT cells for telomeres *IVR* (Figure 5K), *IIIL*, and *VIIL* (data not shown). Spots within 10° of the SPB are obscured by its

(G–I) Histograms for paired telomeres (TEL), sites in the middle of the left arms (MID), and centromeres (CEN) of chromosomes *VII* at 4 hr in sporulation. The CEN and MID sites move slower and without the largest maximum speeds of the telomeres but develop nearly the same bias.

(J) Maximum speed histograms for paired telomeres *IVR* in *ndt80Δ* cells at 4 and 7 hr. Peak 2 persists as cells are held in meiotic prophase.

(K) Maximum speed histograms for telomere *IVR* in WT cells at 4 and 5 hr, combined, where homologous telomeres appear as a single spot (prd) or average either less than 0.4 μm separation (<0.4) or ≥0.4 μm separation (≥0.4) over 1 min. The peak at 2 is apparent in the dataset for telomeres that are nearly paired.

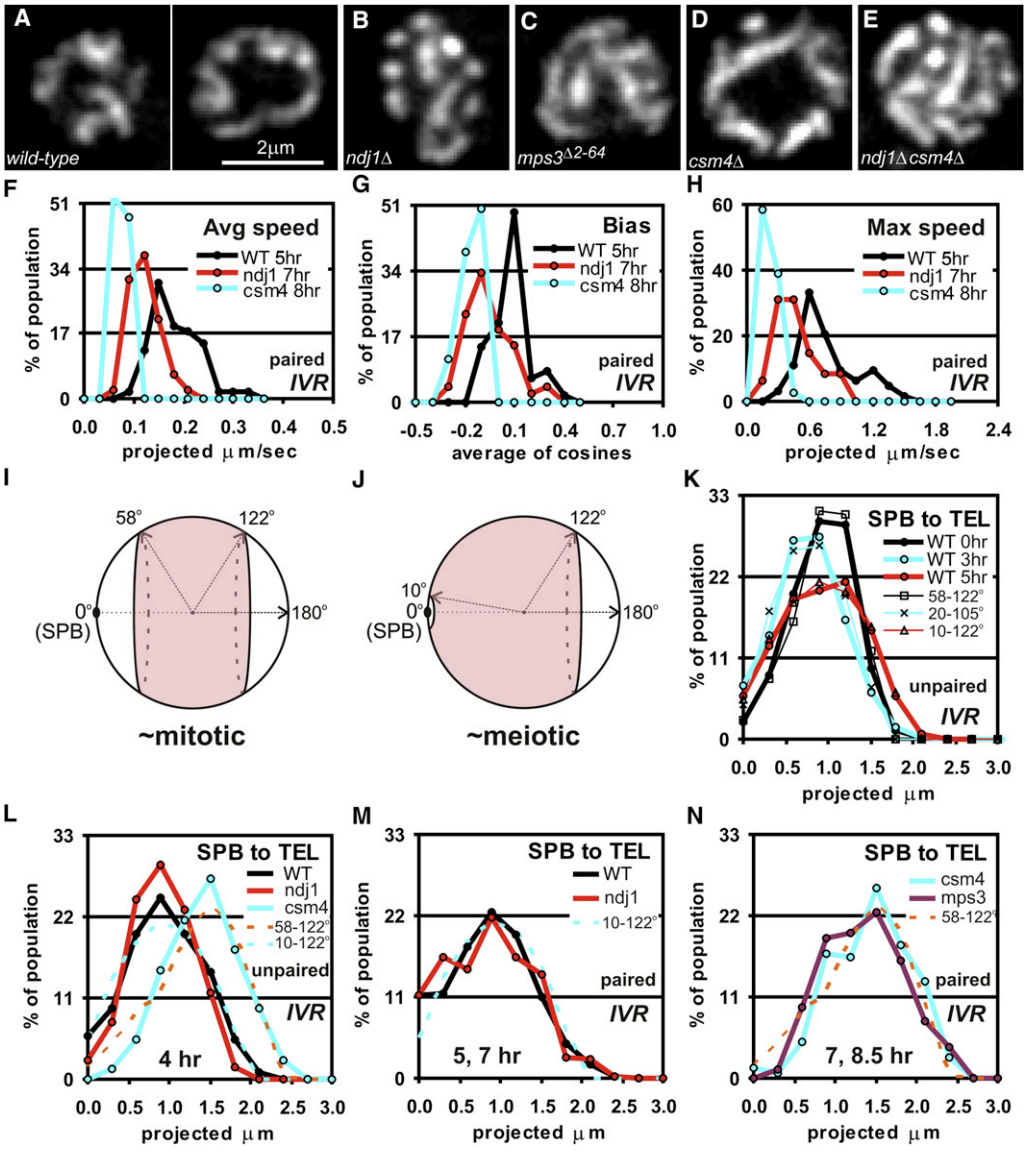

Figure 5. *NDJ1*, *MPS3*, and *CSM4* Are Required for Normal RPMs and Telomere Distribution

(A–E) Single-plane, equatorial confocal images of meiotic prophase nuclei labeled with Rec8-GFP.

(A) Wild-type (WT) chromosomes (at 5 hr) frequently appear excluded from the interior of the nucleus (panel at right).

(B) Chromosomes in *ndj1Δ* (at 7 hr) less often appear excluded from the nucleus interior.

(C) Chromosomes in *mps3*$^{\Delta 2\text{-}64}$ (at 7 hr) generally are distributed as in *ndj1Δ*.

(D) Chromosomes in *csm4Δ* (at 8 hr) generally appear excluded from the nucleus interior.

(E) Chromosomes in *ndj1Δ csm4Δ* (at 8 hr) generally are distributed as in *ndj1Δ*.

(F–H) Histograms of movements of paired telomeres *IVR* in WT, *ndj1Δ* (ndj1), and *csm4Δ* (csm4) (numbers of measurements in Table S1).

(I and J) Diagram of parameters used to model telomere distributions in (F)–(I). Synthetic data were generated to place telomere spots on the surface of randomly oriented spheres and projected onto a square grid that models the camera pixels. Telomeres were restricted to lie between circles defined by their angular displacement from the SPB (the pink areas in the figures; 0°–180° would be unrestricted). Dashed control lines in the following graphs are defined by the two angles and the sphere diameter.

(K–N) Histograms of telomere distances from SPB in WT (WT), *ndj1Δ* (ndj1), *mps3*$^{\Delta 2\text{-}64}$ (mps3), and *csm4Δ* (csm4) in living cells (numbers of measurements in Table S1). Bins are 0.3 μm wide, plotted at the lowest value.

(K) Unpaired telomeres *IVR* at 3 and 5 hr are shifted toward the SPB and distributed more evenly through the nucleus than at 0 hr (controls—2.0 μm [58°–122°], 2.2 μm [20°–105°], and 2.4 μm [10°–122°] spheres).

(L) Unpaired telomeres *IVR* in *csm4Δ* fail to shift toward the SPB at 4 hr (controls—2.4 μm [10°–122°] and 2.8 μm [58°–122°] spheres).

(M) After some delay, paired telomeres *IVR* in *ndj1Δ* (ndj1, 7 hr) become distributed approximately as in WT (5 hr) (control—2.4 μm sphere, 10°–122°).

(N) Paired telomeres in *mps3*$^{\Delta 2\text{-}64}$ (7 hr) and *csm4Δ* (8.5 hr) fail to shift toward the SPB by comparison with WT (H) and with synthetic data (control—2.8 μm sphere, 58°–122°).

fluorescence and telomeres may be excluded from the area from 122°–180° of the SPB by the nucleolus. Paired telomeres differ from unpaired in having higher near-SPB values (compare "WT" in Figures 5L and 5M). Paired telomeres may make more visits to or stay longer at the SPB. Unpaired telomeres show a meiotic distribution in *ndj1Δ* and *mps3*$^{\Delta 2\text{-}64}$ but not in *csm4Δ* (Figure 5L), suggesting that the meiotic distribution of unpaired telomeres does not require RPMs unless the telomeres are firmly anchored. On the other hand, paired telomeres show a meiotic distribution in *ndj1Δ* but not in *mps3*$^{\Delta 2\text{-}64}$ or *csm4Δ* (Figures 5M and 5N), suggesting that the residual RPMs in *ndj1Δ* are necessary and sufficient to maintain the meiotic distribution following synapsis. It is not clear why telomeres fail to occupy the area from ~10°–58° of the SPB in the absence of the RPMs, but exclusion by microtubules emanating from the SPB, which are more prominent at later time points, is possible.

Ndj1p and Mps3p Attach Telomeres to Csm4p

Csm4p accumulates at telomeres in meiotic prophase (Figure 6A). Ndj1p and Mps3p are mutually dependent for their accumulation at telomeres in meiotic prophase (Conrad et al., 2007), and each is required for Csm4p accumulation at telomeres (Figures 6B and 6C). Csm4p remains present in the chromosome spreads in *ndj1Δ* and *mps3*$^{\Delta 2\text{-}64}$, although not at telomeres, presumably because it remains associated with the NE. Conversely, Csm4p is not required for Ndj1p and Mps3p accumulation at telomeres (Figure 6D; Movie S6). In immune co-IP experiments, Mps3p pulls down Ndj1p even in the absence of Csm4p and pulls down Csm4p even in the absence of Ndj1p (Figure 6E), indicating that Csm4p and Mps3p in *ndj1Δ* can interact even though they are not present at telomeres in cytologically detected concentrations.

RPMs Disrupt Nonsynaptic Associations

A possible role for RPMs is to disrupt unstable interactions. As one test of this, we compared the association of homologous telomeres in *ndt80Δ spo11Δ*, where homologs are not tethered by recombinational interactions or synapsis, in the presence and absence (*csm4Δ*) of RPMs. Pairing of telomeres *IVR* at 7 hr was increased ~3-fold in *ndt80Δ spo11Δ csm4Δ* as compared to *ndt80Δ spo11Δ* (Figure 7A). The simplest interpretation of this result is that RPMs generate sufficient force to disrupt associations that are not stabilized by recombination intermediates or by synapsis.

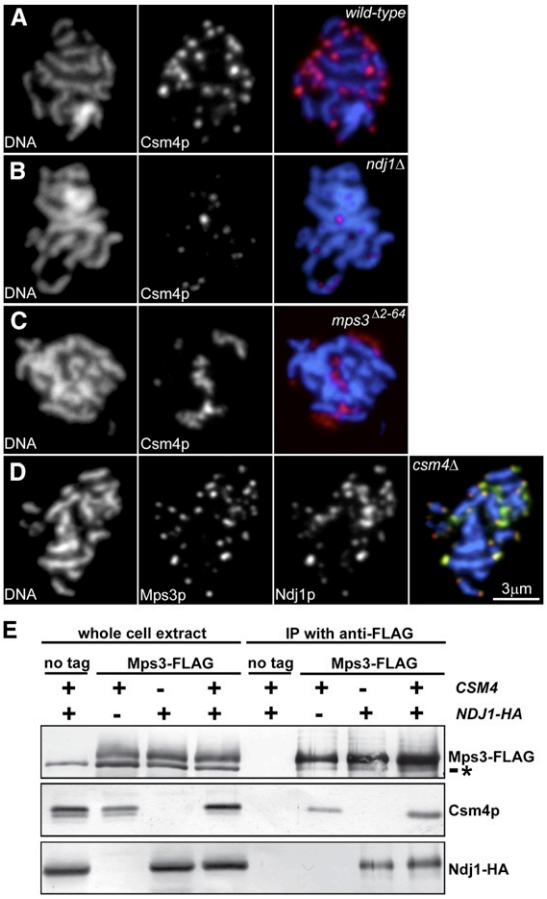

Figure 6. Csm4p Requires, but Is Not Required by, Ndj1p and Mps3p for Normal Levels of Accumulation at Telomeres in Meiotic Prophase

(A–D) Immunofluorescence images of spread preparations of meiotic nuclei labeled with DAPI to visualize chromosomes/DNA (blue in the merged image), anti-GFP to visualize Csm4p-GFP and Mps3p-GFP (red), and anti-HA to visualize Ndj1p-HA (green; magnification bar in D).

(A) Csm4p accumulates at telomeres in wild-type (WT) cells.

(B and C) Csm4p is not evident at telomeres in *ndj1Δ* and *mps3*$^{\Delta 2\text{-}64}$, respectively, though some nucleus-associated accumulations still occur.

(D) Ndj1p and Mps3p accumulate at telomeres in *csm4Δ*.

(E) Western blots of coimmune precipitation results. Immune precipitation of Mps3p-FLAG coprecipitates Csm4p and Ndj1p-HA in extracts from WT cells and coprecipitates Csm4p in extracts from *ndj1Δ* cells. These observations suggest an Mps3p/Csm4p association that persists in the absence of an association with telomeres or with reduced amounts at telomeres in the absence of Ndj1p.

*, nonspecific band.

DISCUSSION

The role of chromosome mechanics in meiotic prophase is to generate crossovers exclusively between homologous pairs of chromosomes. Most prior research has focused on mechanisms that promote connections between chromosomes, in particular on homolog synapsis and allelic recombination. However, recombination between homologous sequences also requires regulation to prevent crossing over between repeated sequences at nonallelic locations and to ensure that each chromosome receives at least one crossover in a location that ensures segregation at anaphase I. RPMs could serve both to moderate homologous interactions (Figure 7D) and to regulate crossover distribution (see below). RPMs may, at different stages or in specific contexts, (1) promote pairing by freeing chromosomes to redistribute within the nucleus, (2) promote bouquet formation, (3) reduce telomere-proximal allelic crossing over, (4) contribute to positive crossover interference, (5) reduce ectopic crossing over, and/or (6) reduce nonrecombinational interactions between bivalents.

Bouquet Genes Promote RPMs

Our results suggest that early in meiotic prophase, Ndj1p stabilizes association of telomeres with Mps3p, thus anchoring

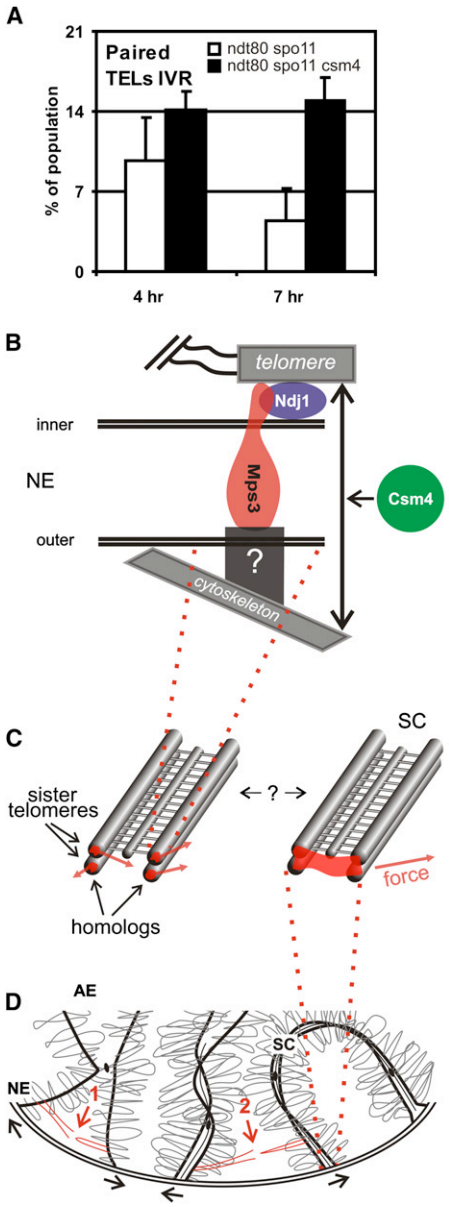

Figure 7. RPMs Break Chromosome Connections in Meiotic Prophase

(A) Telomeres *IVR* association in *ndt80Δ spo11Δ*, which is not promoted by recombination intermediates or synapsis, is reduced as cells are held in meiotic prophase but is maintained in the absence of the RPMs in *ndt80Δ spo11Δ csm4Δ* (4 and 7 hr post-shift into sporulation). Approximately 181 cells were scored for each strain and time point in three independent trials; $\alpha < 5 \times 10^{-3}$ for the 4 versus 7 hr *ndt80Δ spo11Δ* comparison and $\alpha < 10^{-4}$ for the comparison of strains at 7 hr. Error bars represent one standard deviation.

(B) Model for the connection of telomeres to the cytoskeleton in meiotic prophase in *S. cerevisiae*. Ndj1p stabilizes the association of telomeres with Mps3p, which bridges the inner nuclear membrane. The SUN domain of Mps3p interacts with another protein (?), perhaps Mps2p (Jaspersen et al., 2006), to bridge the outer nuclear membrane. Csm4p promotes the link between telomeres and the cytoskeleton.

(C) Alternative models for organization of forces acting on the four telomeres present at the end of a synapsed bivalent. Telomeres may link to the motors individually as on the left, so that sister chromatid cohesion and synaptonemal complex (SC) bind the four chromosomes together, or the link itself may be shared by the four telomeres, as on the right.

(D) Diagram of three pairs of homologous chromosomes anchored at their ends to the nuclear envelope (NE) with loops of chromatin emerging from the axial elements (AE) or, where synapsis has initiated, the lateral elements of each SC. An axial association (Rockmill et al., 1995) at a recombination nodule (small black oval) joins the axes of the pair at left. At 1, RPMs disrupt an early homologous recombination interaction. At 2, RPMs disrupt a homologous recombination interaction between nonhomologs (or, potentially, provide direction for decatenation in concert with topoisomerase activity).

telomeres to the NE. Csm4p, a new component of the bouquet pathway, is required for telomere mobility powered presumably by the actin cytoskeleton (Trelles-Sticken et al., 2005; Koszul et al., 2008) (Figure 7B). Mps2p interacts with the Mps3p SUN domain and with the SPB (Jaspersen et al., 2006) and may contribute to this link. Absent the RPM forces, in *csm4Δ*, telomeres in meiotic prophase are less mobile than in vegetative/premeiotic cells, presumably because they are more strongly anchored. Consistent with this possibility, telomeres are marginally more mobile in *ndj1Δ csm4Δ* than in *csm4Δ* (Table S1). In the absence of Ndj1p, Csm4p, or amino acids 2–64 of Mps3p, paired/synapsed telomeres are less mobile than unpaired telomeres (Table S1), possibly because synapsis generates larger, more rigid assemblies.

Specific RPMs Are Correlated with Early Recombination

On average, RPMs increase as prophase progresses. This could result from the accumulation of more motor molecules or stronger links to the motors, from synapsis of telomeres into a single unit to prevent telomeres of individual chromatids from moving independently and antagonistically (Figure 7C), from resolution of entanglements that inhibit movements, from an increase specifically in a longer range/speed type movement, or from other factors not yet identified. Movements by telomeres at opposite chromosome/bivalent ends could counteract each other, especially for shorter chromosomes, which could account for the slightly reduced RPMs seen for chromosome *III* by comparison with *VII* and *IV* (Table S1).

Analysis of the longest/fastest RPMs reveals a maximum speed peak at 0.75–0.9 μm/s, peak "2," that (1) occurs early in prophase (Figures 3C, 3E, and 3K), (2) requires *SPO11*, *REC8*, and *DMC1* (Figures 4B and 4C), and (3) persists in *zip1Δ* and *ndt80Δ* (Figure 4D). Thus, peak 2 occurs at a time and in the context of early recombination intermediates expected to be present when telomeres form the bouquet and then are dispersed. The majority of peak 2 movements do not appear to be directed specifically toward (or directly away from) the SPB (Figures 1B and 1C and data not shown) and thus are unlikely to represent bouquet formation per se. Peak 2 movements may instead be associated with bouquet dissolution.

The physical basis for the spacing of the maximum speed peaks at ~0.3 μm/s intervals (Figures 3C and 3E) is not clear. One possibility is that the stepwise increases result from the addition of motors acting in series, for example, myosins moving along actin filaments that themselves are being moved by myosins moving along actin filaments.

RPMs May Contribute to Crossover Positioning

Telomere-proximal crossovers are ineffective in orienting chromosomes for disjunction in yeast and in humans (Ross et al., 1996; Hassold and Hunt, 2001). Disruption specifically of nascent recombinational interactions by peak 2 movements, which appear to coincide temporally with crossover designation (Hunter and Kleckner, 2001; Borner et al., 2004; Henderson and Keeney, 2004; Fung et al., 2004), could prevent formation of telomere-proximal crossovers (Figure 7D) and contribute to the normal pattern of crossovers that is known to be altered in *ndj1Δ* (Conrad et al., 1997; Chua and Roeder, 1997; Goldman and Lichten, 2000) and in *csm4Δ* (H. Kosaka, M. Shinohara, and A. Shinohara, personal communication; J. J. Wanat, K. Kim, R. Koszul, S. Zanders, B. Weiner, N. Kleckner, and E. Alani, personal communication). From the perspective that movement disrupts inappropriate crossovers, the bouquet—where movement is reduced and even nonhomologs are held in close proximity—seems likely to generate large numbers of ill-placed crossovers. An interesting possibility is that RPMs, at interstitial locations where the forces are less intense, help trigger crossing over and synapsis. This could account for many of the delays in synapsis and recombination as well as for the alterations in crossover placement and interference seen in the bouquet gene mutants.

RPMs May Reduce Ectopic Recombination

Ectopic recombination is elevated in *ndj1Δ* (Goldman and Lichten, 2000; Schlecht et al., 2004) and *csm4Δ* (H. Kosaka, M. Shinohara, and A. Shinohara, personal communication; J. J. Wanat, K. Kim, R. Koszul, S. Zanders, B. Weiner, N. Kleckner, and E. Alani, personal communication) and may also be elevated in $mps3^{\Delta 2\text{-}64}$, as nondisjunction and premature sister separation are elevated in all three mutants (Conrad et al., 1997; Chua and Roeder, 1997; Conrad et al., 2007; the present work and C.-Y.L. and M.E.D., unpublished data). Elevated missegregation and ectopic recombination have been attributed to the delay in synapsis (Chua and Roeder, 1997; Goldman and Lichten, 2000). However, we have isolated an allele of *MPS3* that has defective RPMs and elevated premature sister separation and nondisjunction in which kinetics of synapsis and exit from prophase appear WT (C.-Y.L. and M.E.D., unpublished data), suggesting that the RPMs may play a direct role in preparing chromosomes for segregation. Synapsis is required for completion of crossing over by the ZMM pathway in *S. cerevisiae* but not for crossovers formed by alternative pathways (de los Santos et al., 2003; Argueso et al., 2004; Fung et al., 2004), which presumably require regulation to avoid generation of ectopic connections. Following completion of synapsis, RPMs could destabilize interactions in these alternative pathways that are not protected by association with the SC (Blat et al., 2002) by pulling apart or scrubbing away inappropriate interactions (Figure 7D). Ultimately, crossover numbers and positions would reflect a balance between DSB numbers and locations, RPMs, synapsis, and regulation imposed at the molecular level (Chambers et al., 1996).

Evolutionary Perspectives

The RPMs reveal a robust association between telomeres and actin-generated forces (Trelles-Sticken et al., 2005; Koszul et al., 2008) that may be a vestige of the contribution of bacterial chromosome segregation mechanisms to the early evolution of eukaryotes (Moller-Jensen et al., 2002; Gitai et al., 2005). A recent proposal that centromeres evolved from telomeres makes a related argument (Villasante et al., 2007). Identification of additional components and of the organization of the RPM machinery may illuminate the evolution of the meiotic bouquet.

In species where meiotic chromosome behavior differs from that in *S. cerevisiae*, for example where there is no obvious bouquet as in worms (Dernburg et al., 1998) and in flies (McKim et al., 1998), RPMs may play a more limited role. Similarly, if crossovers are formed exclusively in the context of the SC, as may be the situation for mouse (see Discussion in Borner et al., 2004), there may be little need for RPMs to reduce ectopic crossovers. Clearly, persistent RPMs cannot take place in *S. pombe* since telomeres remain clustered at the spindle pole throughout meiotic prophase (Chikashige et al., 1994). However, in all organisms there could be a role for RPMs in reducing nonrecombinational associations between nonhomologs, e.g., interlocks (a possibility emphasized in Koszul et al., 2008 and J. J. Wanat, K. Kim, R. Koszul, S. Zanders, B. Weiner, N. Kleckner, and E. Alani, personal communication).

Rapid meiotic chromosome movements in rat (Parvinen and Soderstrom, 1976) and recent descriptions of SUN domain proteins at mouse meiotic telomeres (Ding et al., 2007; Schmitt et al., 2007) suggest that RPMs occur in mammals by similar mechanisms. Differences in RPMs at telomeres or in transmitting the forces to interstitial locations could account for the different patterns of crossovers in human males and females, or among individuals (Cheung et al., 2007), and defects in RPMs could be associated with increased levels of nonallelic homologous recombination and genomic disease (Inoue and Lupski, 2002).

EXPERIMENTAL PROCEDURES

Strains and Assays

Strains and construction are in Table S2. Nondisjunction of chromosome *III* was assayed as described previously (Conrad et al., 1997). Sporulations were carried out in liquid medium for all cytological assays (Kateneva et al., 2005).

Timelapse Microscopy

For timelapse acquisitions, cells from sporulating cultures were concentrated, spread across polyethyleneimine-treated coverslips, then covered with a thin 1% agarose pad to anchor the cells to the coverslip (Yumura et al., 1984). The coverslip was then inverted over a silicone rubber gasket attached to a glass slide, to provide an air space and to prevent drying while imaging. In some experiments, following image acquisition the cell preparations were placed in a humid chamber at 30°C overnight to determine the effects of image acquisition on final levels of sporulation. All timelapse experiments employed an extended depth-of-focus method to acquire fluorescence images (Conchello and Dresser, 2007). Images were made at 27°C using an upright Axioplan 2ie microscope fitted with a 100×, NA1.4 plan-Apo objective (Carl Zeiss MicroImaging), a high-speed switching DG-5 xenon illuminator (Sutter), a CoolSNAP HQ digital camera (Photometrics), and a BNC555 pulse generator (Berkeley Nucleonics) to synchronize camera exposure with focusing movements and illumination. Each image in a timelapse series employed the full camera frame (1392 × 1040 6.45 μm square pixels) to acquire 12-bit images in 250 ms exposures while focus traveled through 10 μm (5 μm on either side of the midfocal plane). Longer travel and exposure times provide better resolved final images, but these conditions clearly revealed the spots of interest and minimized

fading of the fluorescent signals. Fine sampling in the plane of focus (0.0645 μm/pixel) was found to provide better spot discrimination than lower levels of resolution. Following image deconvolution (see Supplemental Experimental Procedures), cells were examined individually to determine the positions of the spots in each timelapse series. The position of each spot was defined as the pixel coordinate nearest the centroid of the brightest local pixels. Positions were assigned automatically by software then edited manually to remove spurious assignments and to correct for overlapping spots; assignment is aided by the summation of intensity that occurs when spots coincide (the images essentially are summed intensity projections, rather than the more familiar maximum intensity projections). Image acquisition, deconvolution, viewing, and quantification were all carried out using custom-written software.

SUPPLEMENTAL DATA

Supplemental Data include Supplemental Experimental Procedures, two tables, one figure, and six figures and can be found with this article online at http://www.cell.com/cgi/content/full/133/7/1175/DC1/.

ACKNOWLEDGMENTS

We thank Ben Fowler (Oklahoma Medical Research Foundation Imaging Facility) and Anton Konovchenko for technical help and Drs. Dean Dawson, Michael Lichten, and Scott Hawley for comments on the manuscript. This work was supported by grants NSF #MCB 98-08000 and OCAST #HR07-026 to MED and by OCAST #HR98-019 to M.N.C.

Received: October 19, 2007
Revised: February 7, 2008
Accepted: April 12, 2008
Published: June 26, 2008

REFERENCES

Allers, T., and Lichten, M. (2001). Differential timing and control of noncrossover and crossover recombination during meiosis. Cell *106*, 47–57.

Argueso, J.L., Wanat, J., Gemici, Z., and Alani, E. (2004). Competing crossover pathways act during meiosis in Saccharomyces cerevisiae. Genetics *168*, 1805–1816.

Beilharz, T., Egan, B., Silver, P.A., Hofmann, K., and Lithgow, T. (2003). Bipartite signals mediate subcellular targeting of tail-anchored membrane proteins in Saccharomyces cerevisiae. J. Biol. Chem. *278*, 8219–8223.

Berg, H.C. (1993). Random Walks in Biology (Princeton, NJ: Princeton University Press).

Bishop, D.K., Park, D., Xu, L., and Kleckner, N. (1992). DMC1: a meiosis-specific yeast homolog of *E. coli* recA required for recombination, synaptonemal complex formation, and cell cycle progression. Cell *69*, 439–456.

Bishop, D.K., and Zickler, D. (2004). Early decision; meiotic crossover interference prior to stable strand exchange and synapsis. Cell *117*, 9–15.

Blat, Y., Protacio, R.U., Hunter, N., and Kleckner, N. (2002). Physical and functional interactions among basic chromosome organizational features govern early steps of meiotic chiasma formation. Cell *111*, 791–802.

Borner, G.V., Kleckner, N., and Hunter, N. (2004). Crossover/noncrossover differentiation, synaptonemal complex formation, and regulatory surveillance at the leptotene/zygotene transition of meiosis. Cell *117*, 29–45.

Bystricky, K., Laroche, T., Van, H.G., Blaszczyk, M., and Gasser, S.M. (2005). Chromosome looping in yeast: telomere pairing and coordinated movement reflect anchoring efficiency and territorial organization. J. Cell Biol. *168*, 375–387.

Cha, R.S., Weiner, B.M., Keeney, S., Dekker, J., and Kleckner, N. (2000). Progression of meiotic DNA replication is modulated by interchromosomal interaction proteins, negatively by Spo11p and positively by Rec8p. Genes Dev. *14*, 493–503.

Chambers, S.R., Hunter, N., Louis, E.J., and Borts, R.H. (1996). The mismatch repair system reduces meiotic homeologous recombination and stimulates recombination-dependent chromosome loss. Mol. Cell. Biol. *16*, 6110–6120.

Cheung, V.G., Burdick, J.T., Hirschmann, D., and Morley, M. (2007). Polymorphic variation in human meiotic recombination. Am. J. Hum. Genet. *80*, 526–530.

Chikashige, Y., Ding, D.Q., Funabiki, H., Haraguchi, T., Mashiko, S., Yanagida, M., and Hiraoka, Y. (1994). Telomere-led premeiotic chromosome movement in fission yeast. Science *264*, 270–273.

Chikashige, Y., Tsutsumi, C., Yamane, M., Okamasa, K., Haraguchi, T., and Hiraoka, Y. (2006). Meiotic proteins bqt1 and bqt2 tether telomeres to form the bouquet arrangement of chromosomes. Cell *125*, 59–69.

Chikashige, Y., Haraguchi, T., and Hiraoka, Y. (2007). Another way to move chromosomes. Chromosoma *116*, 497–505.

Chua, P.R., and Roeder, G.S. (1997). Tam1, a telomere-associated meiotic protein, functions in chromosome synapsis and crossover interference. Genes Dev. *11*, 1786–1800.

Conchello, J.A., and Dresser, M.E. (2007). Extended depth-of-focus microscopy via constrained deconvolution. J. Biomed. Opt. *12*, 064026.

Conrad, M.N., Dominguez, A.M., and Dresser, M.E. (1997). Ndj1p, a meiotic telomere protein required for normal chromosome synapsis and segregation in yeast. Science *276*, 1252–1255.

Conrad, M.N., Lee, C.Y., Wilkerson, J.L., and Dresser, M.E. (2007). MPS3 mediates meiotic bouquet formation in Saccharomyces cerevisiae. Proc. Natl. Acad. Sci. USA *104*, 8863–8868.

de los Santos, T., Hunter, N., Lee, C., Larkin, B., Loidl, J., and Hollingsworth, N.M. (2003). The Mus81/Mms4 endonuclease acts independently of double-Holliday junction resolution to promote a distinct subset of crossovers during meiosis in budding yeast. Genetics *164*, 81–94.

Dernburg, A.F., McDonald, K., Moulder, G., Barstead, R., Dresser, M., and Villeneuve, A.M. (1998). Meiotic recombination in *C. elegans* initiates by a conserved mechanism and is dispensable for homologous chromosome synapsis. Cell *94*, 387–398.

Ding, X., Xu, R., Yu, J., Xu, T., Zhuang, Y., and Han, M. (2007). SUN1 is required for telomere attachment to nuclear envelope and gametogenesis in mice. Dev. Cell *12*, 863–872.

Dresser, M.E., Ewing, D.J., Conrad, M.N., Dominguez, A.M., Barstead, R., Jiang, H., and Kodadek, T. (1997). DMC1 functions in a Saccharomyces cerevisiae meiotic pathway that is largely independent of the RAD51 pathway. Genetics *147*, 533–544.

Fung, J.C., Rockmill, B., Odell, M., and Roeder, G.S. (2004). Imposition of crossover interference through the nonrandom distribution of synapsis initiation complexes. Cell *116*, 795–802.

Gitai, Z., Dye, N.A., Reisenauer, A., Wachi, M., and Shapiro, L. (2005). MreB actin-mediated segregation of a specific region of a bacterial chromosome. Cell *120*, 329–341.

Goldman, A.S., and Lichten, M. (2000). Restriction of ectopic recombination by interhomolog interactions during Saccharomyces cerevisiae meiosis. Proc. Natl. Acad. Sci. USA *97*, 9537–9542.

Hassold, T., and Hunt, P. (2001). To err (meiotically) is human: the genesis of human aneuploidy. Nat. Rev. Genet. *2*, 280–291.

Hayashi, A., Ogawa, H., Kohno, K., Gasser, S.M., and Hiraoka, Y. (1998). Meiotic behaviours of chromosomes and microtubules in budding yeast: relocalization of centromeres and telomeres during meiotic prophase. Genes Cells *3*, 587–601.

Henderson, K.A., and Keeney, S. (2004). Tying synaptonemal complex initiation to the formation and programmed repair of DNA double-strand breaks. Proc. Natl. Acad. Sci. USA *101*, 4519–4524.

Hunter, N., and Kleckner, N. (2001). The single-end invasion: an asymmetric intermediate at the double- strand break to double-holliday junction transition of meiotic recombination. Cell *106*, 59–70.

Inoue, K., and Lupski, J.R. (2002). Molecular mechanisms for genomic disorders. Annu. Rev. Genomics Hum. Genet. *3*, 199–242.

Jaspersen, S.L., Martin, A.E., Glazko, G., Giddings, T.H., Jr., Morgan, G., Mushegian, A., and Winey, M. (2006). The Sad1-UNC-84 homology domain in Mps3 interacts with Mps2 to connect the spindle pole body with the nuclear envelope. J. Cell Biol. *174*, 665–675.

Kateneva, A.V., Konovchenko, A.A., Guacci, V., and Dresser, M.E. (2005). Recombination protein Tid1p controls resolution of cohesin-dependent linkages in meiosis in Saccharomyces cerevisiae. J. Cell Biol. *171*, 241–253.

Keeney, S., Giroux, C.N., and Kleckner, N. (1997). Meiosis-specific DNA double-strand breaks are catalyzed by Spo11, a member of a widely conserved protein family. Cell *88*, 375–384.

Kleckner, N., Zickler, D., Jones, G.H., Dekker, J., Padmore, R., Henle, J., and Hutchinson, J. (2004). A mechanical basis for chromosome function. Proc. Natl. Acad. Sci. USA *101*, 12592–12597.

Klein, F., Laroche, T., Cardenas, M.E., Hofmann, J.F., Schweizer, D., and Gasser, S.M. (1992). Localization of RAP1 and topoisomerase II in nuclei and meiotic chromosomes of yeast. J. Cell Biol. *117*, 935–948.

Klein, F., Mahr, P., Galova, M., Buonomo, S.B., Michaelis, C., Nairz, K., and Nasmyth, K. (1999). A central role for cohesins in sister chromatid cohesion, formation of axial elements, and recombination during yeast meiosis. Cell *98*, 91–103.

Koszul, R., Kim, K., Prentiss, M., Kleckner, N., and Kameoka, S. (2008). Actin-mediated motion of meiotic chromosomes. Cell *133*, this issue, 1188–1201.

McKim, K.S., Green-Marroquin, B.L., Sekelsky, J.J., Chin, G., Steinberg, C., Khodosh, R., and Hawley, R.S. (1998). Meiotic synapsis in the absence of recombination. Science *279*, 876–878.

Miki, F., Kurabayashi, A., Tange, Y., Okazaki, K., Shimanuki, M., and Niwa, O. (2004). Two-hybrid search for proteins that interact with Sad1 and Kms1, two membrane-bound components of the spindle pole body in fission yeast. Mol. Genet. Genomics *270*, 449–461.

Miki, F., Okazaki, K., Shimanuki, M., Yamamoto, A., Hiraoka, Y., and Niwa, O. (2002). The 14-kDa dynein light chain-family protein Dlc1 is required for regular oscillatory nuclear movement and efficient recombination during meiotic prophase in fission yeast. Mol. Biol. Cell *13*, 930–946.

Moller-Jensen, J., Jensen, R.B., Lowe, J., and Gerdes, K. (2002). Prokaryotic DNA segregation by an actin-like filament. EMBO J. *21*, 3119–3127.

Parvinen, M., and Soderstrom, K.O. (1976). Chromosome rotation and formation of synapsis. Nature *260*, 534–535.

Penkner, A., Tang, L., Novatchkova, M., Ladurner, M., Fridkin, A., Gruenbaum, Y., Schweizer, D., Loidl, J., and Jantsch, V. (2007). The nuclear envelope protein Matefin/SUN-1 is required for homologous pairing in *C. elegans* meiosis. Dev. Cell *12*, 873–885.

Rabitsch, K.P., Toth, A., Galova, M., Schleiffer, A., Schaffner, G., Aigner, E., Rupp, C., Penkner, A.M., Moreno-Borchart, A.C., Primig, M., et al. (2001). A screen for genes required for meiosis and spore formation based on whole-genome expression. Curr. Biol. *11*, 1001–1009.

Rockmill, B., Sym, M., Scherthan, H., and Roeder, G.S. (1995). Roles for two RecA homologs in promoting meiotic chromosome synapsis. Genes Dev. *9*, 2684–2695.

Ross, L.O., Maxfield, R., and Dawson, D. (1996). Exchanges are not equally able to enhance meiotic chromosome segregation in yeast. Proc. Natl. Acad. Sci. USA *93*, 4979–4983.

Scherthan, H., Wang, H., Adelfalk, C., White, E.J., Cowan, C., Cande, W.Z., and Kaback, D.B. (2007). Chromosome mobility during meiotic prophase in Saccharomyces cerevisiae. Proc. Natl. Acad. Sci. USA *104*, 16934–16939.

Schlecht, H.B., Lichten, M., and Goldman, A.S. (2004). Compartmentalization of the yeast meiotic nucleus revealed by analysis of ectopic recombination. Genetics *168*, 1189–1203.

Schmitt, J., Benavente, R., Hodzic, D., Hoog, C., Stewart, C.L., and Alsheimer, M. (2007). Transmembrane protein Sun2 is involved in tethering mammalian meiotic telomeres to the nuclear envelope. Proc. Natl. Acad. Sci. USA *104*, 7426–7431.

Shimanuki, M., Miki, F., Ding, D.Q., Chikashige, Y., Hiraoka, Y., Horio, T., and Niwa, O. (1997). A novel fission yeast gene, kms1+, is required for the formation of meiotic prophase-specific nuclear architecture. Mol. Gen. Genet. *254*, 238–249.

Sym, M., Engebrecht, J.A., and Roeder, G.S. (1993). ZIP1 is a synaptonemal complex protein required for meiotic chromosome synapsis. Cell *72*, 365–378.

Trelles-Sticken, E., Dresser, M.E., and Scherthan, H. (2000). Meiotic telomere protein Ndj1p is required for meiosis-specific telomere distribution, bouquet formation and efficient homologue pairing. J. Cell Biol. *151*, 95–106.

Trelles-Sticken, E., Adelfalk, C., Loidl, J., and Scherthan, H. (2005). Meiotic telomere clustering requires actin for its formation and cohesin for its resolution. J. Cell Biol. *170*, 213–223.

Villasante, A., Abad, J.P., and Mendez-Lago, M. (2007). Centromeres were derived from telomeres during the evolution of the eukaryotic chromosome. Proc. Natl. Acad. Sci. USA *104*, 10542–10547.

White, E.J., Cowan, C., Cande, W.Z., and Kaback, D.B. (2004). In vivo analysis of synaptonemal complex formation during yeast meiosis. Genetics *167*, 51–63.

Xu, L., Ajimura, M., Padmore, R., Klein, C., and Kleckner, N. (1995). NDT80, a meiosis-specific gene required for exit from pachytene in Saccharomyces cerevisiae. Mol. Cell. Biol. *15*, 6572–6581.

Yumura, S., Mori, H., and Fukui, Y. (1984). Localization of actin and myosin for the study of ameboid movement in Dictyostelium using improved immunofluorescence. J. Cell Biol. *99*, 894–899.

Zickler, D. (2006). From early homologue recognition to synaptonemal complex formation. Chromosoma *115*, 158–174.

Zickler, D., and Kleckner, N. (1998). The leptotene-zygotene transition of meiosis. Annu. Rev. Genet. *32*, 619–697.